A Stream-wise Blind Selected Mapping Technique for Low-PAPR Multi-user MIMO Transmission

(Invited Paper)

Amnart Boonkajay[†] and Fumiyuki Adachi[††]
Research Organization of Electrical Communication (ROEC), Tohoku University
2-1-1 Katahira, Aoba-ku, Sendai, Miyagi, 980-8577 Japan
E-mail: [†]amnart@riec.tohoku.ac.jp, [††]adachi@ecei.tohoku.ac.jp

***Abstract*—Peak-to-average power ratio (PAPR) of transmit waveform becomes higher when transmit filtering and/or precoding are employed. In this paper, we introduce a PAPR reduction scheme called selected mapping without side information transmission (called blind SLM) for both orthogonal frequency division multiplexing (OFDM) and single-carrier (SC) signals. Firstly, we review the proposed blind SLM techniques, considering both single-input single output (SISO) and space-time block coded transmit diversity (STBC-TD). Then, a blind SLM technique for multi-user multiple-input multiple-output (MU-MIMO) transmission with minimum mean-square error (MMSE) filtering and singular value decomposition (SVD), called MMSE-SVD, is introduced. To realize a simple data detection without side-information in MU-MIMO, we recommend that the phase rotation sequence multiplication should be applied to transmit data streams before applying the transmit filtering (called stream-wise SLM). At the receiver, the phase rotation sequence estimation is done for each users data streams after applying the receive filtering. Simulation results confirm that the stream-wise blind SLM for MMSE-SVD can reduce the PAPR of transmit waveforms without degrading bit-error rate (BER).**

***Index Terms*—OFDM, single carrier, MU-MIMO, STBC, PAPR, selected mapping**

I. Introduction

High peak-to-average power ratio (PAPR) signal remains a major problem in the fifth-generation (5G) mobile communications since it degrades energy efficiency (EE) of user equipment (UE), especially when operating at high carrier frequency e.g. millimeter wave [1]. Single-carrier (SC) waveform is well-known as a low-PAPR waveform compared to orthogonal frequency division multiplexing (OFDM) waveform [2]. OFDM and SC can be combined with single-user space-time block coded transmit diversity (STBC-TD) [3] or with multi-user multiple-input multiple-output (MU-MIMO) transmission [4] to boost up the spectrum efficiency (SE). MU-MIMO using minimum mean-square error (MMSE) filtering and singular value decomposition (SVD), called MMSE-SVD, was introduced recently [5], where it can achieve better bit-error rate (BER) than zero-forcing (ZF) based receive filtering. However, PAPR increases when the transmit filtering and/or precoding are employed even in SC transmission [6], indicating that PAPR reduction is necessary. Among various PAPR techniques, selected mapping (SLM) [7] is well-known as an efficient PAPR reduction scheme with less computational complexity than partial transmit sequence (PTS) [8]. SLM selects a waveform having the lowest PAPR among many candidates obtained from phase rotations. Meanwhile, its main drawback is side information transmission, which degrades the SE especially in MIMO systems.

In this paper, SLM without side information transmission (called blind SLM) for both OFDM and SC transmissions are introduced. Firstly, we review the previous blind SLM techniques which are mostly based on OFDM transmission and introduce our blind SLM techniques which are compatible with both OFDM and SC, considering single-input single-output (SISO) and STBC-TD. Then, we introduce a blind SLM technique for MMSE-SVD, in which the phase rotation is multiplied to data streams prior to transmit filtering (called stream-wise SLM). Phase rotation estimation can be employed to each UE's data stream after receive filtering and no major changes on MMSE-SVD filters implementation is required. Performance evaluation of the stream-wise blind SLM for MMSE-SVD is carried out by computer simulation, where OFDM is used in downlink transmission (base station (BS) to UEs) and SC is for uplink (UEs to BS) transmission similar to the current LTE-Advanced system. It is shown that the blind SLM can achieve low-PAPR transmission without BER degradation when the received signal power is sufficiently high.

II. Overview of Blind SLM and Its Application to STBC-TD

Blind SLM techniques for OFDM has been widely studied, such as scrambling [9] and modified block code [10], but they still need to transmit small amount of redundant bits. A blind SLM for OFDM based on maximum likelihood (ML) phase rotation estimation [11] is attractive since it can achieve similar BER as that of perfect side information knowledge, but [11] considers a continuous set of phase rotation and becomes impractical. Blind SLM for SISO SC using a discrete set of phase rotation and ML-based phase rotation estimation was proposed in [12], which is also compatible with OFDM transmission. Its extensions for STBC-TD with and without transmit frequency-domain equalization (Tx-FDE) were discussed in [13] and [14].

Here, we describe the concept of blind SLM, including phase rotation sequence selection and estimation, then briefly introduce its applications to STBC-TD. In addition, we assume that the single-user STBC-TD with Tx-FDE, where the number of BS antennas (N_{BS}) can be arbitrary, is used in the OFDM

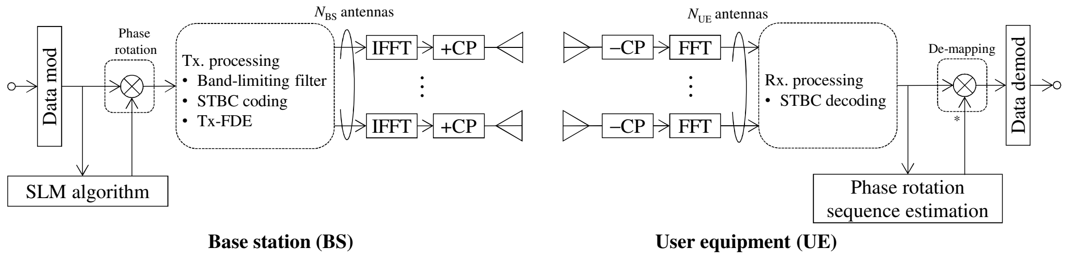

(a) OFDM downlink (with Tx-FDE)

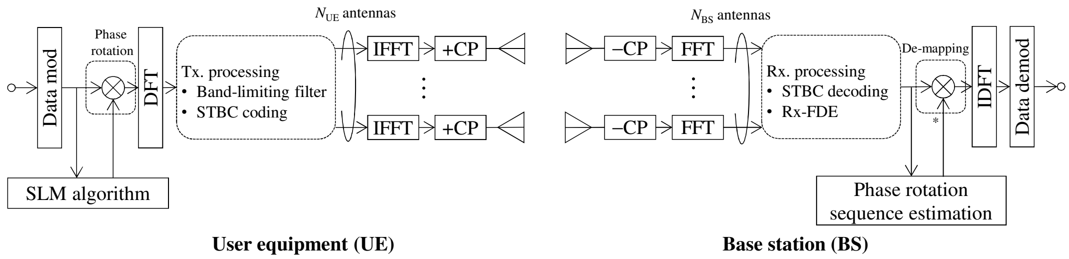

(b) SC uplink (without Tx-FDE)

Fig. 1. Transceiver model with STBC-TD and blind SLM.

downlink, while the STBC-TD without Tx-FDE is adopted in the SC uplink. The system model is depicted by Fig. 1. For simplicity, we describe only the signal representation of STBC-TD. The representation for SISO can be obtained by setting all STBC parameters, i.e. the number of BS antennas (N_{BS}) and UE antennas (N_{UE}), J, Q, and coding rate R_{STBC} to be 1.

A. SLM algorithm

Assuming that a time-domain transmit waveform is $\{s(n); n = 0 \sim N_c - 1\}$, PAPR is calculated over a V-times oversampled block and is given by

$$\mathrm{PAPR}(\{s(n)\}) = \frac{\max\{|s(n)|^2, n=0, \frac{1}{V}, \frac{2}{V}, \ldots, N_c - 1\}}{\frac{1}{N_c}\sum_{n=0}^{N_c-1}|s(n)|^2}. \quad (1)$$

It is seen in Fig. 1 that the phase rotation is carried out prior to transmit signal processing. The j-th block of an N_c-length data sequence $\{d_j(n); n = 0 \sim N_c - 1, j = 0 \sim J-1\}$ is multiplied with the selected phase rotation sequence $\{\Phi_{\hat{m}}(n); n = 0 \sim N_c - 1\}$, yielding the rotated block $\{d_{j,\hat{m}}(n); n = 0 \sim N_c - 1, j = 0 \sim J-1\}$. In the SC uplink, $\{d_{j,\hat{m}}(n)\}$ is transformed into frequency-domain component block $\{D_{j,\hat{m}}(k); k = 0 \sim N_c-1\}$ by N_c-point discrete Fourier transform (DFT). In the OFDM downlink, we simply obtain $\{D_{j,\hat{m}}(k); k = 0 \sim N_c - 1\} = \{d_{j,\hat{m}}(k)\}$. Then, transmit signal processings e.g. STBC coding and Tx-FDE are applied to $\{D_{j,\hat{m}}(k)\}$ to obtain the frequency-domain transmit signal at the n_t-th transmit antenna ($n_t = 0 \sim N_{\mathrm{BS}} - 1$ for downlink and $n_t = 0 \sim N_{\mathrm{UE}} - 1$ for uplink) and the q-th timeslot as $\{S^{\hat{m}}_{n_t,q}(k); k = 0 \sim N_c - 1\}$. In addition, its corresponding time-domain waveform after applying inverse DFT (IDFT) is defined as $\{s^{\hat{m}}_{n_t,q}(n); n = 0 \sim N_c - 1\}$.

In SC uplink using STBC-TD without Tx-FDE, it is known that the PAPR of signals before and after STBC coding are the same. This is because the STBC coding employs only complex conjugate operations [3,14]. Therefore, we can select an individual phase rotation sequence for each of the j-th block. The selected sequence $\{\Phi_{\hat{m}(j)}(n)\}$, with the corresponding sequence index $\hat{m}(j)$, is determined by

$$\hat{m}(j) = \arg\min_{m=0\sim M-1}\left(\mathrm{PAPR}(\{\Phi_m(n)d_j(n)\})\right), \quad (2)$$

where $\{\Phi_m(n); n = 0 \sim N_c - 1, m = 0 \sim M - 1\}$ is the m-th phase sequence in a codebook and is generated randomly as $\Phi_m(n) \in \{e^{j0}, e^{j2\pi/3}, e^{j4\pi/3}\}$, except the first sequence is defined as $\{\Phi_0(n) = e^{j0}; n = 0 \sim N_c - 1\}$ [12-14].

However, (2) is not available for STBC-TD with Tx-FDE since the signals before and after Tx-FDE have different PAPR. In this case, a selection criterion which minimizes the maximum PAPR value (called mini-max criterion) among all N_{BS} transmit antennas and Q timeslots is used. A common phase rotation for all J blocks is defined by $\{\Phi_{\hat{m}}(n)\}$, with the corresponding index $\hat{m}$, where its selection criterion is

$$\hat{m} = \arg\min_{m=0\sim M-1}\left(\max_{\substack{n_{\mathrm{BS}}=0\sim N_{\mathrm{BS}}-1\\ q=0\sim Q-1}} \mathrm{PAPR}(\{s^{m}_{n_{\mathrm{BS}},q}(n)\})\right), \quad (3)$$

The selection criterion in (3) is sub-optimal and hence the PAPR slightly increases when N_{BS} increases. However, it can keep the phase rotation estimation simple and no major changes on Tx-FDE weight calculation is required.

B. Phase rotation sequence estimation

Phase rotation sequence estimation is employed after the receive signal processing such as STBC decoding. It is based on Euclidean distance calculation between the de-mapped signal and original constellations. The phase rotation sequence associated with the de-mapped signal having the minimum Euclidean distance is selected. Assuming that the j-th time-domain received block before de-mapping is $\{\hat{d}_j(n); n = 0 \sim$

$N_c-1, j=0\sim J-1\}$, the phase rotation sequence estimation can be expressed as

$$\tilde{m}=\arg\min_{\substack{m=0\sim M-1\\ \mathbb{C}\in\Psi_{\mathrm{mod}}}}\left(\epsilon=\sum_{n=0}^{N_c-1}\left|\Phi_m^*(n)\hat{d}_j(n)-\mathbb{C}\right|^2\right), \quad (4)$$

where Ψ_{mod} is the original data-modulated constellation (e.g. QAM mapping). The estimation in (4) can be used in both STBC-TD with and without Tx-FDE.

III. Application of Blind SLM to MMSE-SVD

Our proposed blind SLM techniques in [12-14] have not yet considered their extension to MU-MIMO. A conventional SLM for OFDM-MIMO with spatial multiplexing was proposed in [15], which employs phase rotation individually at each transmit antenna (called antenna-wise SLM) and can achieve the same PAPR as SISO. A sub-optimal SLM which applies phase rotation directly to the transmit antenna emitting high-PAPR signal (called directed SLM) was proposed in [16]. Meanwhile, [15-16] did not consider MU-MIMO and the use of transmit filtering. More importantly, it is difficult to conduct signal detection without side-information in MMSE-SVD when the SLMs in [15-16] are used since the phase rotation estimation at the receiver needs to consider all possible filter coefficients. To realize low-PAPR MMSE-SVD transmission and a simple data detection without side-information, a stream-wise blind SLM is introduced in this section.

Here, we also consider OFDM for the downlink and SC for the uplink, same as in Sect. II. MMSE-SVD system model consisting of U UEs, each equipped with N_{UE} antennas, and a single BS equipped with N_{BS} antennas is illustrated in Fig. 2. The stream-wise blind SLM is also equipped. We assume that each UE sends/receives $G=N_{\mathrm{UE}}$ data streams and adaptive rank/modulation control (ARMC) [6] is not considered.

A. OFDM downlink

OFDM downlink MMSE-SVD system with stream-wise blind SLM is depicted by Fig. 2(a). At the BS, information sequence to be transmitted to the u-th UE is data-modulated into G streams of N_c-length block $\{\mathbf{D}_u(k); k=0\sim N_c-1\}$ with $\mathbf{D}_u(k)=[D_{u,0}(k),\ldots,D_{u,g}(k),\ldots,D_{u,G-1}(k)]^T$. Assuming that the UEs employ eigenmode reception [17], the transmit frequency component $N_{\mathrm{BS}}\times 1$ vector at the k-th subcarrier can be expressed by the following matrix form.

$$\mathbf{S}_{\mathrm{DL}}(k)=\sqrt{\frac{2E_s}{T_s}}\mathbf{W}_{T,\mathrm{DL}}(k)\left(\Phi_{\hat{m}}(k)\mathbf{D}_{\mathrm{DL}}(k)\right), \quad (5)$$

where $\mathbf{D}_{\mathrm{DL}}(k)=[\mathbf{D}_0(k),\ldots,\mathbf{D}_u(k),\ldots,\mathbf{D}_{U-1}(k)]^T$. E_s and T_s are symbol energy and symbol duration, respectively. The transmit filtering matrix $\mathbf{W}_{T,\mathrm{DL}}(k)$ with dimension of $N_{\mathrm{BS}}\times(U\cdot G)$ is determined by [14]

$$\begin{aligned}&\mathbf{W}_{T,\mathrm{DL}}(k)\\&=[\mathbf{W}_{T,\mathrm{DL},0}(k),\ldots,\mathbf{W}_{T,\mathrm{DL},u}(k),\ldots,\mathbf{W}_{T,\mathrm{DL},U-1}(k)]\\&=\left(\mathbf{U}_{\mathrm{DL}}^H(k)\mathbf{H}(k)\right)^H\\&\times\left(\left(\mathbf{U}_{\mathrm{DL}}^H(k)\mathbf{H}(k)\right)\left(\mathbf{U}_{\mathrm{DL}}^H(k)\mathbf{H}(k)\right)^H+\left(\frac{N_0}{E_s}\right)\mathbf{I}_{U\cdot G}\right)^{-1}\mathbf{P}^{1/2}(k)\end{aligned} \quad (6)$$

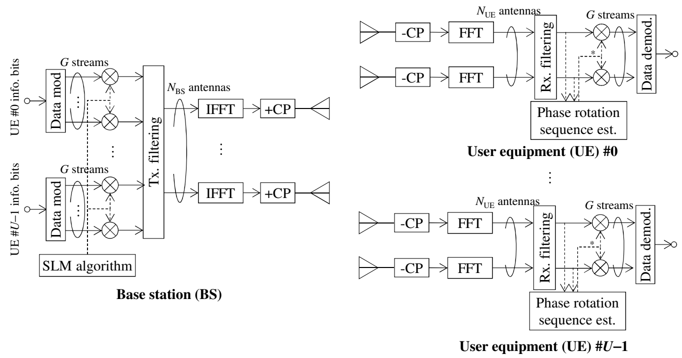

(a) OFDM downlink

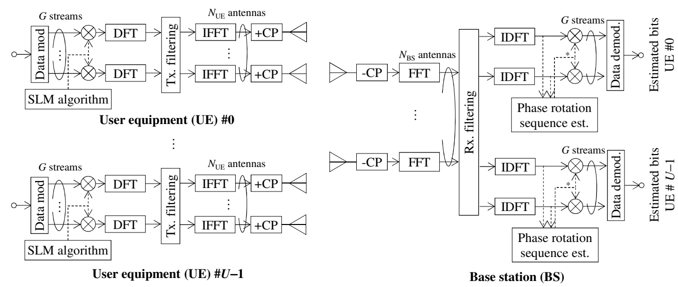

(b) SC uplink

Fig. 2. MMSE-SVD system models with blind SLM.

Note that $\mathbf{A}^H$ represents a Hermitian transpose of $\mathbf{A}$ and N_0 is one-sided noise power spectrum density. $\mathbf{H}(k)=[\mathbf{H}_0^T(k),\ldots,\mathbf{H}_u^T(k),\ldots,\mathbf{H}_{U-1}^T(k)]^T$ is $(U\cdot N_{\mathrm{UE}})\times N_{\mathrm{BS}}$ matrix representing the downlink channel between BS and U UEs, in which $\mathbf{H}_u(k)$ representing an $N_{\mathrm{BS}}\times N_{\mathrm{UE}}$ uplink channel matrix between the u-th UE and the BS, and its transpose $\mathbf{H}_u^T(k)$ is the downlink channel matrix of the BS and the u-th UE. $\mathbf{U}_{\mathrm{DL}}(k)=diag\{\mathbf{U}_{\mathrm{DL},0}(k),\ldots,\mathbf{U}_{\mathrm{DL},u}(k),\ldots,\mathbf{U}_{\mathrm{DL},U-1}(k)\}$ with an $N_{\mathrm{UE}}\times N_{\mathrm{UE}}$ unitary matrix $\mathbf{U}_{\mathrm{DL},u}(k)$ is obtained by applying SVD to $\mathbf{H}_u^T(k)$ as follow.

$$\mathbf{H}_u^T(k)=\mathbf{U}_{\mathrm{DL},u}(k)\mathbf{\Lambda}_{\mathrm{DL},u}^{1/2}(k)\mathbf{V}_{\mathrm{DL},u}^H(k), \quad (7)$$

where $\mathbf{\Lambda}_{\mathrm{DL},u}^{1/2}(k)$ is a $G\times G$ matrix whose the g-th diagonal element, $\Lambda_{\mathrm{DL},u,g}^{1/2}(k), g=0\sim G-1$, contains an eigenvalue of the g-th eigenmode. $\mathbf{P}(k)$ is a $U\cdot G\times U\cdot G$ diagonal matrix representing water-filling power allocation, whose the $(u\cdot g)$-th diagonal element is given by

$$P_{u,g}(k)=\max\left(\frac{1}{\sqrt{\mu_u}}-\frac{1}{(\frac{E_s}{N_0})\Lambda_{\mathrm{DL},u,g}(k)},0\right). \quad (8)$$

Note that μ_u is chosen for satisfying the power constraint.

In (5), the selected phase sequence $\{\Phi_{\hat{m}}(k); k=0\sim N_c-1\}$ is multiplied to all data streams $\{\mathbf{D}_u(k)\}$. Here, the selection is done based on mini-max criterion, which minimizes the maximum PAPR among N_{BS} antennas, and is expressed by

$$\hat{m}=\arg\min_{m=0\sim M-1}\left(\max_{n_{\mathrm{BS}}=0\sim N_{\mathrm{BS}}-1}\mathrm{PAPR}(\{s_{n_{\mathrm{BS}}}^m(n)\})\right), \quad (9)$$

where $\{s^m_{n_{\rm BS}}(n); n = 0 \sim N_c - 1\}$ is the time-domain transmit signal at the $n_{\rm BS}$-th antenna and is obtained by applying N_c-point IDFT to $\{\mathbf{S}^m_{\rm DL}(k) = \mathbf{W}_{T,\rm DL}(k)\left(\Phi_m(k)\mathbf{D}_{\rm DL}(k)\right); k = 0 \sim N_c - 1\}$. A codebook of $\{\Phi_m(k)\}$ is already defined in Sect. II. In addition, it is possible to select an individual phase rotation sequence for the g-th data stream from available B sequences, but we have confirmed by computer simulation that it achieves the same PAPR as selecting a common sequence for all $U \cdot G$ streams from $M = B^{(U\cdot G)}$ available sequences.

At the u-th UE, the cyclic prefix (CP)-removed received signal blocks through $N_{\rm UE}$ antennas are transformed into frequency domain by N_c-point DFT. The frequency-domain received signal vector at the k-th subcarrier, $\mathbf{R}_u(k)$, is

$$\mathbf{R}_u(k) = \mathbf{H}^T_u(k)\mathbf{S}_{\rm DL}(k) + \mathbf{Z}_u(k), \tag{10}$$

where $\mathbf{Z}_u(k)$ is an $N_{\rm UE} \times 1$ additive white Gaussian noise (AWGN) vector whose element has zero-mean and variance of $2N_0/T_s$. The received data streams before de-mapping and data de-modulation $\{\hat{\mathbf{D}}_u(k); k = 0 \sim N_c - 1\}$ with $\hat{\mathbf{D}}_u(k) = [\hat{D}_{u,0}(k), \ldots, \hat{D}_{u,g}(k), \ldots, \hat{D}_{u,G-1}(k)]^T$ are obtained by simply applying SVD filtering and are given by

$$\begin{array}{rcl}\hat{\mathbf{D}}_u(k) & = & \mathbf{W}_{R,\rm DL,u}(k)\mathbf{R}_u(k) \\ & = & \mathbf{U}^H_{{\rm DL},u}(k)\mathbf{R}_u(k)\end{array}. \tag{11}$$

In general, if the SLM is applied at the transmitter, the receiver needs to conduct de-mapping before data de-modulation, which is expressed by

$$\tilde{\mathbf{D}}_u(k) = \Phi^*_{\hat{m}}(k)\hat{\mathbf{D}}_u(k). \tag{12}$$

However, (12) requires side-information transmission to know $\hat{m}$. Here, we applies the phase rotation sequence estimation separately for each UEs received signal. The received candidate corresponding to the v-th de-mapping sequence is obtained as $\{\hat{\mathbf{D}}^v_u(k) = \Phi^*_v(k)\hat{\mathbf{D}}_u(k); k = 0 \sim N_c - 1\}$ where $\hat{\mathbf{D}}^v_u(k) = [\hat{D}^v_{u,0}(k), \ldots, \hat{D}^v_{u,g}(k), \ldots, \hat{D}^v_{u,G-1}(k)]^T$. The Euclidean distance between $\{\hat{\mathbf{D}}^v_u(k)\}$ and the closet constellations is computed. The estimated phase rotation sequence of the u-th user $\{\Phi_{\tilde{m}}(k)\}$, with the index $\tilde{m}$, is found by

$$\tilde{m} = \arg \min_{\substack{v=0\sim M-1 \\ \mathbb{C}\in\Psi_{\rm mod}}} \left(\epsilon = \sum_{g=0}^{G-1}\sum_{n=0}^{N_c-1}\left|\hat{D}^v_{u,g}(k) - \mathbb{C}\right|^2\right), \tag{13}$$

Finally, the received data streams before de-modulation can be obtained by replacing $\tilde{m}$ instead of $\hat{m}$ in (12).

B. SC uplink

SC uplink MMSE-SVD system with stream-wise blind SLM is depicted by Fig. 2(b). At the u-th UE, information sequence is data-modulated into G streams of N_c-length data-modulated block $\{\mathbf{d}_u(n); n = 0 \sim N_c - 1\}$ with $\mathbf{d}_u(n) = [d_{u,0}(n), \ldots, d_{u,g}(n), \ldots, d_{u,G-1}(n)]^T$. Each stream is transformed into frequency-domain components block by DFT, yielding the frequency-domain components block $\{\mathbf{D}_u(k); k = 0 \sim N_c - 1\}$ as

$$D_{u,g}(k) = \frac{1}{\sqrt{N_c}}\sum_{n=0}^{N_c-1}\Phi_{\hat{m}(u)}(n)d_{u,g}(n)\exp(-i2\pi\frac{kn}{N_c}). \tag{14}$$

where $i = \sqrt{-1}$. The frequency-domain component vector at the k-th subcarrier, $\mathbf{D}_u(k)$, is then multiplied by an $N_{\rm UE} \times G$ transmit filtering matrix $\mathbf{W}_{T,{\rm UL},u}(k)$, obtaining the frequency-domain signal transmitted from $N_{\rm UE}$ antennas of the u-th UE, $\mathbf{S}_u(k) = [S_{u,0}(k), \ldots, S_{u,n_{\rm UE}}(k), \ldots, S_{u,N_{\rm UE}-1}(k)]^T$, as

$$\mathbf{S}_u(k) = \sqrt{\frac{2E_s}{T_s}}\mathbf{W}_{T,{\rm UL},u}(k)\mathbf{D}_u(k), \tag{15}$$

where $\mathbf{W}_{T,{\rm UL},u}(k)$ is described in [5] and is given by

$$\mathbf{W}_{T,{\rm UL},u}(k) = \mathbf{V}_{{\rm UL},u}(k)\mathbf{P}^{1/2}_u(k), \tag{16}$$

where $\mathbf{V}_{{\rm UL},u}(k)$ is an $N_{\rm UE} \times N_{\rm UE}$ unitary matrix whose columns consisting of right singular vector of $\mathbf{H}_u(k)$ as

$$\mathbf{H}_u(k) = \mathbf{U}_{{\rm UL},u}(k)\mathbf{\Lambda}^{1/2}_{{\rm UL},u}(k)\mathbf{V}^H_{{\rm UL},u}(k). \tag{17}$$

Here, $\mathbf{\Lambda}^{1/2}_{{\rm UL},u}(k)$ is a $G \times G$ matrix whose the g-th diagonal element, $\Lambda^{1/2}_{{\rm UL},u,g}(k), g = 0 \sim G - 1$, contains an eigenvalue of the g-th eigenmode. $\mathbf{P}_u(k)$ is a $G \times G$ diagonal matrix representing MMSE power allocation, whose the g-th diagonal element is given by

$$P_{u,g}(k) = \max\left(\frac{1}{\sqrt{\mu_u}\sqrt{\frac{E_s}{N_0}\Lambda_{{\rm UL},u,g}(k)}} - \frac{1}{\frac{E_s}{N_0}\Lambda_{{\rm UL},u,g}(k)}, 0\right). \tag{18}$$

The frequency-domain signals $\{\mathbf{S}_u(k); k = 0 \sim N_c - 1\}$ is transformed back into time domain by N_c-point IDFT, yielding the time-domain blocks to be transmitted through $N_{\rm UE}$ antennas $\{\mathbf{s}_u(n); n = 0 \sim N_c - 1\}$ with $\mathbf{s}_u(n) = [s_{u,0}(n), \ldots, s_{u,n_{\rm UE}}(n), \ldots, s_{u,N_{\rm UE}-1}(n)]^T$ as

$$s_{u,n_{\rm UE}}(n) = \frac{1}{\sqrt{N_c}}\sum_{k=0}^{N_c-1}S_{u,n_{\rm UE}}(k)\exp(i2\pi\frac{kn}{N_c}). \tag{19}$$

Here, the phase rotation selection criterion for SC uplink is similar to that of OFDM downlink, i.e. mini-max criterion. The selected phase rotation sequence for the u-th user $\{\Phi_{\hat{m}(u)}(n)\}$, with the corresponding index $\hat{m}(u)$, is given by

$$\hat{m}(u) = \arg \min_{m=0\sim M-1}\left(\max_{n_{\rm UE}=0\sim N_{\rm UE}-1}{\rm PAPR}\left(\{s^m_{u,n_{\rm UE}}(n)\}\right)\right). \tag{20}$$

Here, $\{s^m_{u,n_{\rm UE}}(n); n = 0 \sim N_c - 1\}$ represents the transmit waveform at the $n_{\rm UE}$-th antenna and is obtained from $\{\mathbf{d}^m_u(n) = \Phi_m(n)\mathbf{d}_u(n); n = 0 \sim N_c - 1\}$. Note that the selected phase rotation sequence can be different for U UEs since the transmit waveforms from each UE are independent.

At the BS, the CP-removed received signal blocks through $N_{\rm BS}$ antennas are transformed into frequency domain by N_c-point DFT. The frequency-domain received signal vector at the k-th subcarrier, $\mathbf{R}(k)$, is expressed by

$$\begin{aligned}\mathbf{R}(k) &= \sum_{u=0}^{U-1}\mathbf{H}_u(k)\mathbf{S}_u(k) + \mathbf{Z}(k) \\ &= \sqrt{\tfrac{2E_s}{T_s}}(\mathbf{H}_{total}(k)\mathbf{W}_{total}(k))\begin{bmatrix}\mathbf{D}_0(k) \\ \vdots \\ \mathbf{D}_{U-1}(k)\end{bmatrix} + \mathbf{Z}(k)\end{aligned}, \tag{21}$$

where $(\mathbf{H}_0(k)\mathbf{W}_{T,\mathrm{UL},0}(k)\ldots\mathbf{H}_{U-1}(k)\mathbf{W}_{T,\mathrm{UL},U-1}(k))$ is defined as an $N_{\mathrm{BS}} \times (G \cdot U)$ equivalent channel matrix $\mathbf{H}_{total}(k)\mathbf{W}_{total}(k)$. $\mathbf{Z}(k)$ is an $N_{\mathrm{BS}} \times 1$ AWGN vector. The frequency-domain output blocks $\{\hat{\mathbf{D}}(k); k = 0 \sim N_c - 1\}$ with $\hat{\mathbf{D}}(k) = [\hat{\mathbf{D}}_0(k), \ldots, \hat{\mathbf{D}}_u(k), \ldots, \hat{\mathbf{D}}_{U-1}(k)]^T$ and $\hat{\mathbf{D}}_u(k) = [\hat{D}_{u,0}(k), \ldots, \hat{D}_{u,g}(k), \ldots, \hat{D}_{u,G-1}(k)]^T$ are obtained by applying MMSE filtering, i.e. $\hat{\mathbf{D}}(k) = \mathbf{W}_{R,\mathrm{UL}}(k)\mathbf{R}(k)$, where $\mathbf{W}_{R,\mathrm{UL}}(k)$ is a $(U \cdot G) \times N_{\mathrm{BS}}$ matrix and is given by

$$\begin{aligned}&\mathbf{W}_{R,\mathrm{UL}}(k)\\&= (\mathbf{H}^T(k)\mathbf{W}_{T,\mathrm{UL}}(k))^H\\&\times \left((\mathbf{H}^T(k)\mathbf{W}_{T,\mathrm{UL}}(k))(\mathbf{H}^T(k)\mathbf{W}_{T,\mathrm{UL}}(k))^H + \left(\frac{E_s}{N_0}\right)^{-1}\right)^{-1}\end{aligned} \tag{22}$$

where $\mathbf{W}_{T,\mathrm{UL}}(k) = diag\{\mathbf{W}_{T,\mathrm{UL},0}(k), \ldots, \mathbf{W}_{T,\mathrm{UL},U-1}(k)\}$. Finally, $\{\hat{\mathbf{D}}(k)\}$ are transformed back into time domain by N_c-point IDFT, yielding the time-domain received blocks before data de-modulation $\{\hat{\mathbf{d}}(n); n = 0 \sim N_c - 1\}$, with $\hat{\mathbf{d}}(n) = [\hat{\mathbf{d}}_0(n), \ldots, \hat{\mathbf{d}}_u(n), \ldots, \hat{\mathbf{d}}_{U-1}(n)]^T$ and $\hat{\mathbf{d}}_u(n) = [\hat{d}_{u,0}(n), \ldots, \hat{d}_{u,g}(n), \ldots, \hat{d}_{u,G-1}(n)]^T$.

Here, the phase rotation sequence estimation is carried out for each UEs received data streams. the time-domain received candidate corresponding to the v-th de-mapping sequence is obtained as $\{\hat{\mathbf{d}}_u^v(n) = \Phi_v^*(n)\hat{\mathbf{d}}_u(n); n = 0 \sim N_c - 1\}$, with $\hat{\mathbf{d}}_u^v(n) = [\hat{d}_{u,0}^v(n), \ldots, \hat{d}_{u,g}^v(n), \ldots, \hat{d}_{u,G-1}^v(n)]^T$. The estimated phase rotation sequence of the u-th UE $\{\Phi_{\tilde{m}(u)}(k)\}$, with the index $\tilde{m}(u)$, is determined by

$$\tilde{m}(u) = \arg \min_{\substack{v=0\sim M-1\\ \mathbb{C}\in\Psi_{\mathrm{mod}}}} \left(\epsilon = \sum_{g=0}^{G-1}\sum_{n=0}^{N_c-1}\left|\hat{d}_{u,g}^v(n) - \mathbb{C}\right|^2\right). \tag{23}$$

The estimation in (13) and (23) can be done by either exhaustive search (maximum-likelihood; ML) [12-14] or 2-step estimation using Viterbi algorithm [18]. Finally, the received data streams before de-modulation can be obtained by $\tilde{\mathbf{d}}_u(n) = \Phi_{\tilde{m}(u)}^*(n)\hat{\mathbf{d}}_u(n)$.

IV. Performance Evaluation

Simulation parameters are summarized in Table I. Perfect channel state information (CSI) and uncoded transmission are considered for simplicity. Performance of the proposed stream-wise SLM is carried out and is compared with that of the antenna-wise SLM with perfect $N_t \log_2(M)$-bit side information detection [15].

A. PAPR

PAPR performance is evaluated by measuring the PAPR value at complementary cumulative distribution function (CCDF) equals 10^{-3}, called $\mathrm{PAPR}_{0.1\%}$. Fig. 3 shows $\mathrm{PAPR}_{0.1\%}$ versus M of OFDM downlink and SC uplink MU-MIMO using MMSE-SVD transmit/receive filtering. The data modulation scheme is set to be 16QAM. $\mathrm{PAPR}_{0.1\%}$ of the conventional SISO-OFDM without SLM (10.7 dB) and the conventional SISO-SC without SLM (8.7 dB) are also plotted for comparison.

Firstly, it is seen when M=1 (no SLM) that the use of SVD filtering with joint transmit/receive MMSE power allocation drastically increases the PAPR of SC uplink waveform [6],

TABLE I
Simulation parameters.

Modulation	Data modulation	16QAM, 64QAM
	FFT/IFFT block size	N_c = 128
	Cyclic prefix length	N_g = 16
User equipment	Tx/Rx filter	SVD
	No. of UE antennas	N_{UE} = 2
	No. of streams	G = N_{UE} = 2
Blind SLM parameter	Phase sequence type	Random polyphase
	No. of sequences	M = 1~512
	Phase sequence estimation method	Maximum-likelihood
Channel	Fading type	Frequency-selective block Rayleigh
	Power delay profile	symbol-spaced 16-path uniform
Base station	No. of BS antennas	N_{BS} = 4
	Tx/Rx filter	MMSE

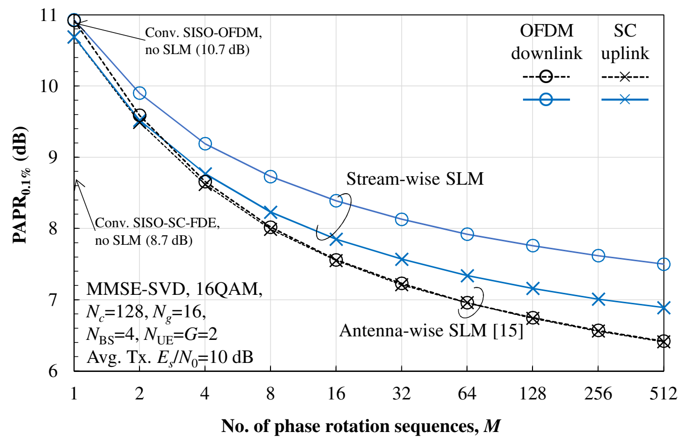

Fig. 3. $\mathrm{PAPR}_{0.1\%}$ versus M.

where there is no major difference in PAPR of SISO OFDM and OFDM downlink with MMSE-SVD. PAPR can be reduced by increasing M in both the antenna-wise SLM and the stream-wise SLM, but the PAPR of MMSE-SVD using the stream-wise SLM is higher than that of the antenna-wise SLM. This is because the mini-max criterion in (9) and (20) decreases the degree of freedom in waveform candidate generation [13]. Assuming that M=256, the stream-wise SLM can lower the PAPR by 3.7 dB and 3.3 dB in SC uplink and OFDM downlink, respectively, which are only 0.5 dB and 1.0 dB higher than that of the antenna-wise SLM (i.e., only 0.5 dB and 1.0 dB higher than the optimal solution).

In addition, we have also evaluated the PAPR of SC-MU-MIMO with MMSE-SVD transmit/receive filterings using 64QAM, but the results are not shown in this paper since they are very similar to those of 16QAM.

B. BER

Figs. 4(a) and 4(b) show the uncoded average BER of OFDM downlink and SC uplink MU-MIMO using MMSE-SVD and the stream-wise blind SLM as a function of average total transmit E_s/N_0, respectively. The MU-MIMO system configuration $(U \times N_{\mathrm{UE}}, N_{\mathrm{BS}})$ equals $(2 \times 2, 4)$. BER of the MU-MIMO using MMSE-SVD without SLM is also plotted

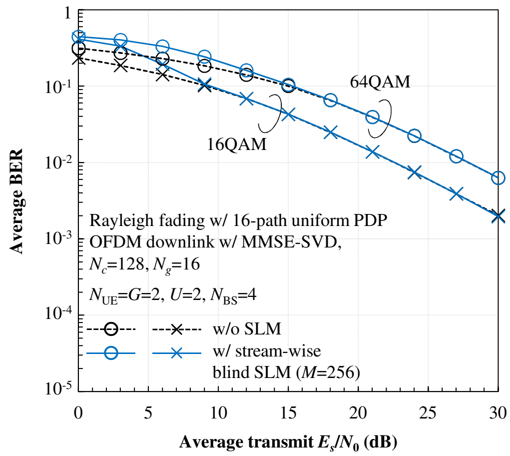

(a) OFDM downlink

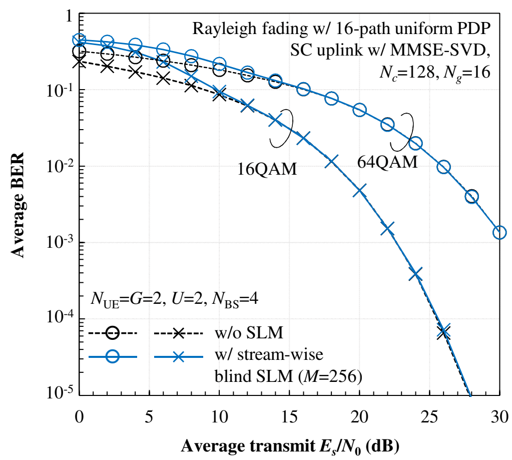

(b) SC uplink

Fig. 4. BER performance of MMSE-SVD with blind SLM.

for comparison. The number of phase rotation sequences is M=256. In addition, performance comparison of MMSE-SVD and receive ZF has been examined in [5], hence the BER of MU-MIMO with ZF filtering is not discussed here. It is seen from Figs. 4(a) and 4(b) that there is no major difference among BER performances of transmission without SLM, and the transmission with stream-wise blind SLM although there is no side-information sharing, especially when the average transmit E_s/N_0 is sufficiently high (i.e. higher than 10 dB). From Figs. 3 and 4, we can conclude that our proposed stream-wise SLM can realize a simple data detection without side information in MU-MIMO, while the PAPR reduction capability is only 1.0 dB apart from the optimal solution.

V. Conclusion

In this paper, firstly, the principle of blind SLM and its application to STBC-TD were overviewed. Then, the stream-wise blind SLM for MMSE-SVD in both OFDM downlink and SC uplink was proposed. The sub-optimal blind SLM employs phase rotation sequence multiplication to transmit data streams and prior to transmit filtering. The phase rotation sequence estimation for stream-wise blind SLM can be carried out similar to that of SISO blind SLM. Computer simulation results confirmed that the stream-wise blind SLM can lower the PAPR of the OFDM downlink and SC uplink MMSE-SVD by 3.3 dB and 3.7 dB, respectively, when M=256, which is only 1.0 dB and 0.5 dB apart from the optimal values. It is also shown that no significant BER degradation occurs even though there is no side-information transmission.

Acknowledgment

This paper includes a part of results of “The research and development project for realization of the fifth-generation mobile communications system,” commissioned to Tohoku University by The Ministry of Internal Affairs and Communications (MIC), Japan.

References

[1] 5GMF White Paper, *5G Mobile Communications Systems for 2020 and Beyond*, Ver. 1.01, Jul. 2016.

[2] H. G. Myung et al., “Single Carrier FDMA for Uplink Wireless Transmission,” *IEEE Veh. Technol. Mag.*, Vol. 1, No. 3, pp. 30-38, Sept. 2006.

[3] S. M. Alamouti, “A Simple Transmit Diversity Technique for Wireless Communications,” *IEEE J. Select. Areas. Commun.*, Vol. 16, No. 8, pp. 1451-1458, Oct. 1998.

[4] D. Gesbert et al., “Shifting the MIMO Paradigm,” *IEEE Signal Process. Mag.*, Vol. 24, No. 5, pp. 36-46, Oct. 2007.

[5] S. Kumagai and F. Adachi, “Joint Tx/Rx MMSE Filtering for Single-Carrier MU-MIMO Uplink,” *Proc. IEEE VTS Asia Pacific Wireless Commun. Symp. (APWCS2015)*, Singapore, Aug. 2015.

[6] S. Kumagai et al., “Joint Tx/Rx MMSE Filtering for Single-Carrier MIMO Transmission,” *IEICE Trans. Commun.*, Vol. E97-B, No. 9, pp. 1967-1976, Sept. 2014.

[7] R. W. Bauml et al., “Reducing the Peak-to-Average Power Ratio of Multicarrier Modulation by Selected Mapping,” *IEEE Electron. Lett.*, Vol. 32, No. 22, pp. 2056-2057, Oct. 1996.

[8] R. J. Baxley and G. T. Zhou, “Comparison of Selected Mapping and Partial Transmit Sequence for Crest Factor Reduction in OFDM,” *Proc. IEEE Military Commun. Conf. (MILCOM2006)*, Washington D.C., USA, Oct. 2006.

[9] M. Breiling et al., “SLM Peak-Power Reduction without Explicit Side Information,” *IEEE Commun. Lett.*, Vol. 5, No. 6, pp. 239-241, Jun. 2001.

[10] N. Carson and T. A. Gulliver, “PAPR Reduction of OFDM using Selected Mapping, Modified RA Codes and Clipping,” *Proc. IEEE Veh. Technol. Conference (VTC2002-Fall)*, Vancouver, Canada, Sept. 2002.

[11] A. D. S. Jayalath and C. Tellambura, “SLM and PTS Peak Power Reduction of OFDM Signals without Side Information,” *IEEE Trans. Wireless Commun.*, Vol. 4, No. 5, pp. 2006-2013, Sept. 2005.

[12] A. Boonkajay and F. Adachi, “A Blind Polyphase Time-Domain Selected Mapping for Filtered Single-Carrier Signal Transmission,” *Proc. IEEE Veh. Technol. Conference (VTC2016-Fall)*, Montreal, Canada, Sept. 2016.

[13] A. Boonkajay and F. Adachi, “PAPR Reduction for STBC Transmit Diversity with Transmit FDE using Blind Selected Mapping,” *to be presented at IEEE VTS Asia Pacific Wireless Commun. Symp. (APWCS2017)*, Incheon, Korea, Aug. 2017.

[14] F. Adachi et al., “Cooperative Distributed Antenna Transmission for 5G Mobile Communications Network,” *IEICE Trans. Commun.*, Vol. E100-B, No. 8, pp. 1190-1204, Aug. 2017.

[15] M. S. Baek et al., “Semi-Blind Channel Estimation and PAR Reduction for MIMO-OFDM System with Multiple Antennas,” *IEEE Trans. Broadcast.*, Vol. 50, Issue 4, pp. 414-424, Dec. 2004.

[16] R. F. H. Fischer and M. Hoch, “Directed Selected Mapping for Peak-to-Average Power Ratio Reduction in MIMO OFDM,” *IEE Electron. Lett.*, Vol. 42, No. 22, pp. 1289-1290, Oct. 2006.

[17] W. Liu et al., “SVD-assisted Multiuser Transmitter and Multiuser Detector Design for MIMO Systems,” *IEEE Trans. Veh. Technol.*, Vol. 58, No. 2, pp. 1016-1021, Feb. 2009.

[18] A. Boonkajay and F. Adachi, “2-Step Signal Detection for Blind Time-Domain Selected Mapping,” *Proc. IEEE Int. Symp. on Personal Indoor and Mobile Radio Commun. (PIMRC2017)*, Montreal, Canada, Oct. 2017.